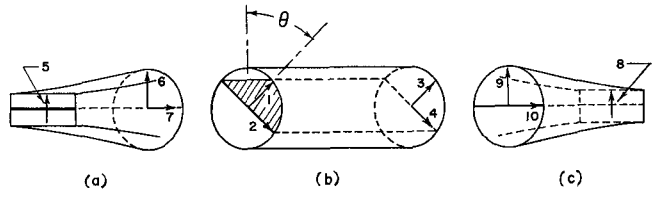

Fig. 1. Rotary-vane attenuator represented by cascade of three networks. Transitions are three-ports while the circular section is a four-port. Absorbing vanes lie in horizontal plane of transitions and in the 2–4 plane of circular section.

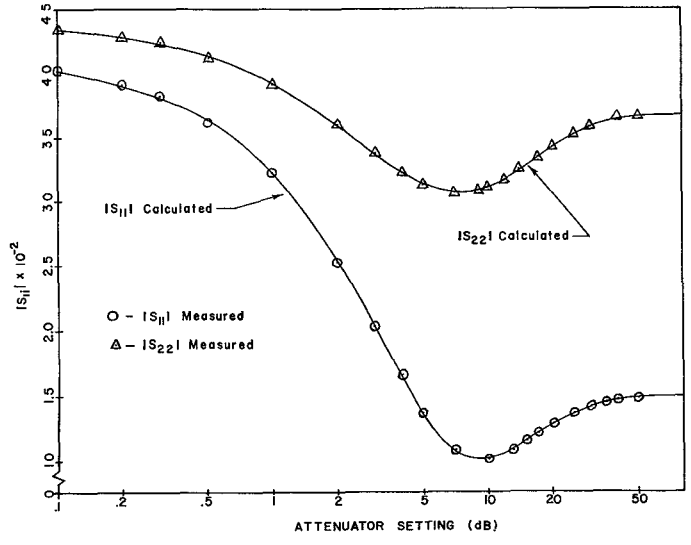

Fig. 2. Measured and calculated magnitudes of reflection coefficients of FXR X164A X-band attenuator.

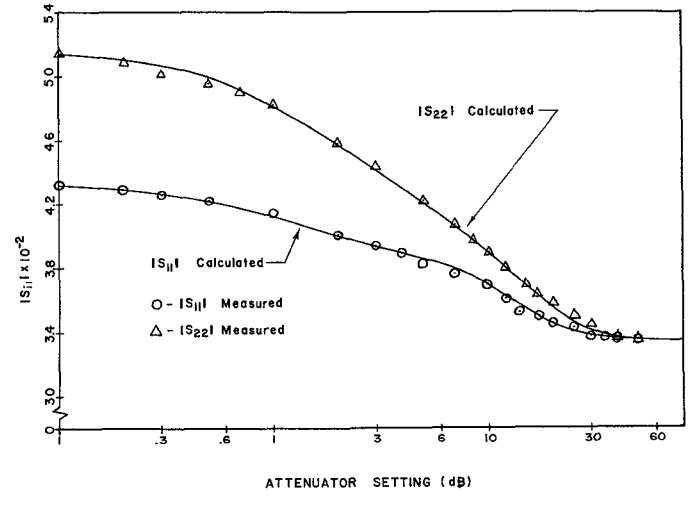

Fig. 3. Measured and calculated magnitudes of reflection coefficients of FXR K164AF K-band attenuator.

TABLE I

ATTENUATOR CONSTANTS

	FXR X164A X-Band Attenuator		FXR K164AF K-Band Attenuator	
	S_{11}	S_{22}	S_{11}	S_{22}
A_{ii}	0.0412	0.0439	0.0436	0.0520
B_{ii}	$0.0560\ e^{-3.16}$	$0.0679\ e^{-23\ 66}$	$0.0580\ e^{-j3.75}$	$0.0334\ e^{-72\ 46}$
C_{ii}	$0.0125\ e^{-74\ 04}$	$0.00927\ e^{-75.06}$	$0.0135\ e^{-75.10}$	$0.0106\ e^{-21\ 58}$

the phase of S_{ii} was not measured, it is believed unlikely that it would not similarly agree with theory.

J. D. HOLM
D. L. JOHNSON
K. S. CHAMPLIN
Dept. of Elec. Engrg.
University of Minnesota
Minneapolis, Minn.

REFERENCES

[1] C. G. Montgomery, R. H. Dicke, and E. M. Purcell, *Principles of Microwave Circuits*. New York: McGraw-Hill, 1948, pp. 148–151.
[2] E. F. Barnett, "A precison waveguide attenuator which obeys a mathematical law," *Hewlett-Packard J.*, vol. 6, pp. 1–2, January 1955.
[3] K. S. Champlin, J. D. Holm, J. Holm-Kennedy, and D. B. Armstrong, "Reflection coefficient bridge," *IEEE Trans. on Microwave Theory and Techniques*, (submitted for publication).
[4] R. W. Beatty, "Mismatch errors in the measurement of ultrahigh-frequency and microwave variable attenuators," *J. Res. Nat. Bur. Stand.* vol. 52, pp. 7–9, January 1954.
[5] G. F. Engen and R. W. Beatty, "Microwave attenuation measurements with accuracies from 0.0001 to 0.06 decibel over a range of 0.01 to 50 decibels," *J. Res. Nat. Bur. Stand.*, vol. 64C, pp. 139–145, April–June 1960.
[6] D. A. Ellerbruch, "Evaluation of a microwave phase measurment system," *J. Res. Nat. Bur. Stand.* vol. 69C, pp. 55–65, January–March 1965.
[7] G. F. Engen and R. W. Beatty, "Microwave reflectometer techniques," *IRE Trans. on Microwave Theory and Techniques*, vol. MTT-7, pp. 351–355, July 1959.

Temperature Dependence of Composite Coaxial Resonators

Under certain circumstances, it is necessary to construct a composite coaxial resonator using inner and outer conductors having different thermal expansion coefficients. This may be required for mechanical reasons or as a means of adjusting the resonator temperature stability. This correspondence describes an analysis of such a resonator as well as some experimental results.

The resonant frequency of a quarter-wavelength capacitively loaded line is given by

$$\frac{10^{-12}}{\omega CZ} = \tan 2\pi L/\lambda \qquad (1)$$

where

ω = resonant frequency, rad/s
C = loading capacitance, pF
Z = impedance of coaxial line, ohms
L = length of inner conductor, cm
λ = wavelength at resonance, cm.

Equation (1) is transcendental and can be solved by graphical means[1] if the loading capacitance is known, by letting

$$Y_{11} = \tan 2\pi L/\lambda \qquad (2)$$

and

$$Y_{12} = \frac{\lambda\epsilon}{2\pi vCZ} \qquad (3)$$

Manuscript received June 16 1966; revised September 8, 1966.

[1] G. K. Megla, *Dezimeterwellentechnik*. Berlin: Veb Verlag Technik, 1961, p. 189.

where

$$\epsilon = 855.5 \text{ pF/cm}$$

$$v = 3 \times 10^{10} \text{ cm/s}.$$

Plotting Y_{11} and Y_{12} versus λ yields two families of curves (Fig. 1) with simultaneous solutions at points of intersection.

A section view of a quarter-wavelength resonator is shown in Fig. 2. The loading capacitances are indicated. In many cases, the resonator is designed such that the parallel-plate capacitance C_{pp} is small; consequently, the end-wall fringing capacitance C_{fe} is negligible. Under these conditions, the side-wall fringing capacitance C_{fs} is significant in all cases, and is the predominant factor in deviations from exact quarter-wavelength operation. Consequently, only this capacitance will be considered in the analysis.

It is possible to obtain an estimate of the side-wall fringing capacitance by adopting results developed for a slightly different application.[2,3,4] The longitudinal section of the resonator given in Fig. 2 (neglecting the end wall) is seen to be similar to a cross-sectional view of a rectangular bar between ground planes as shown in the inset in Fig. 3. This gives the fringing capacitance per unit length. To adapt this to the coaxial situation, the circumference of the inner conductor becomes the length along which fringing occurs.

For the composite resonator, where the inner and outer conductor are constructed from different materials, the loading capacitance temperature dependence, in general, is a complex function of both material expansions. The fringing capacitance of Fig. 3 is given analytically as

$$C_{fs1} = \frac{0.0885\epsilon_r}{\pi} [2(t_1) \ln (t_1 + 1) - (t_1 - 1) \ln (t_1^2 - 1)]2\pi a, \text{ pF/cm} \quad (4)$$

where

$$t_1 = \frac{1}{1 - a/b}$$

ϵ_r = relative permittivity.

After subjection to a temperature change ΔT, the new fringing capacitance C_{fs2} is given as

$$C_{fs2} = \frac{0.0885\epsilon_r}{\pi} \cdot [2(t_2) \ln (t_2 + 1) - (t_2 - 1) \ln (t_2^2 - 1)]2\pi a \cdot (1 + \alpha(a)\Delta T), \text{ pF/cm} \quad (5)$$

where

$$t_2 = \frac{1}{1 - \dfrac{a(1 + \alpha(a)\Delta T)}{b(1 + \alpha(b)\Delta T)}}$$

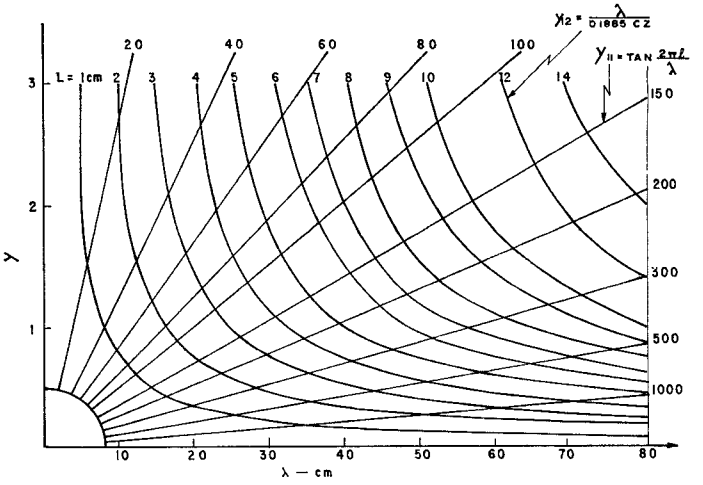

Fig. 1. Solutions to $\frac{10^{-12}}{\omega CZ} = \tan 2\pi L/\lambda$.

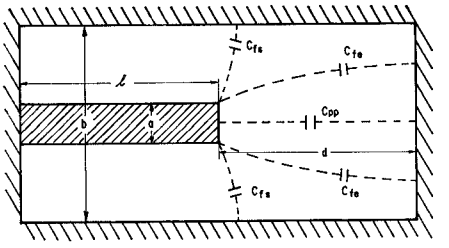

Fig. 2. Coaxial resonator loading capacitances.

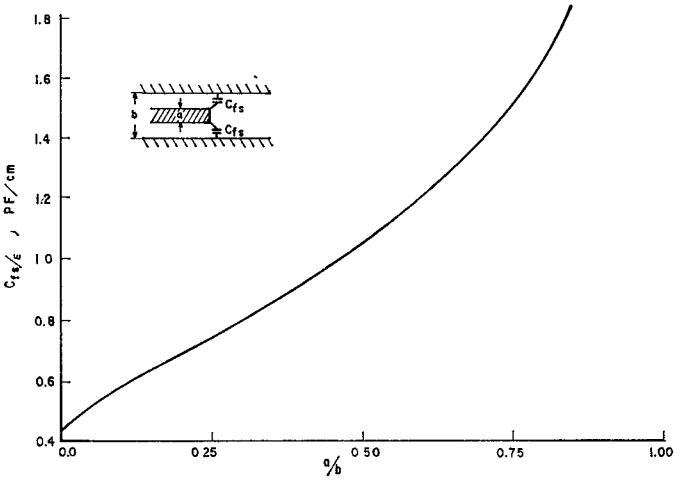

Fig. 3. Normalized fringing capacitance (after Cohn, Getsinger).

$\alpha(a)$ = expansion coefficient of inner conductor

$\alpha(b)$ = expansion coefficient of outer conductor.

This is a complex dependence on the expansion of both materials. Note, however, that when, $\alpha(a) = \alpha(b)$, the equation reduces to a simple dependence on $(1 + \alpha\Delta T)$.

For the ideal case of an open-circuited resonator, the characteristic impedance of the coaxial structure has no effect on the resonant wavelength. As soon as the line is loaded, the impedance enters the determination of resonance as given by (1).

At the initial temperature, the impedance of the coaxial line is given by

$$Z_1 = 60 \ln b/a \text{ (ohms)}. \quad (6)$$

At a temperature differing by ΔT, the new impedance is given by

$$Z_2 = 60 \ln \frac{b(1 + \alpha(b)\Delta T)}{a(1 + \alpha(a)\Delta T)} \text{ (ohms)}. \quad (7)$$

The change in impedance as a function of temperature can be shown to be

$$Z = 60(\alpha(b) - \alpha(a))\Delta T. \quad (8)$$

The resonance condition for a loaded quarter-wavelength line has been given as

[2] W. J. Getsinger, "Coupled rectangular bars between parallel-plates," *IRE Trans. on Microwave Theory and Techniques*, vol. MTT-10, pp. 65–72, January 1962.

[3] G. L. Matthaei, L. Young, and E. M. T. Jones, *Microwave Filters, Impedance Matching Networks, and Coupling Structures*, New York: McGraw-Hill, 1964, p. 190.

[4] S. B. Cohn, "Problems in strip transmission lines," *IRE Trans. on Microwave Theory and Techniques*, vol. MTT-3, pp. 119–126, March 1955.

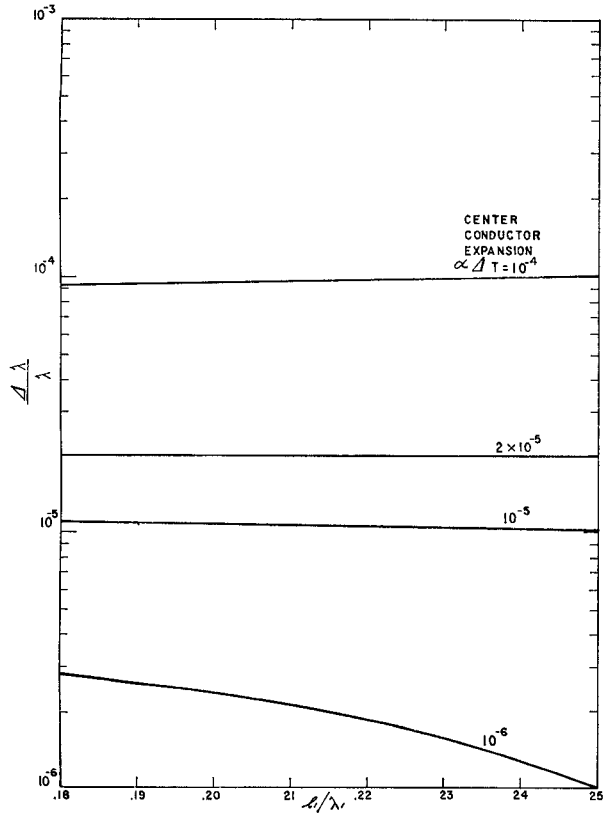

Fig. 4. Stability versus loading for composite coaxial resonator. Brass outer conductor for various inner conductor expansions: $b/a = 3.6$ $a = 0.9$ cm. Outer conductor expansion: 2×10^{-5}.

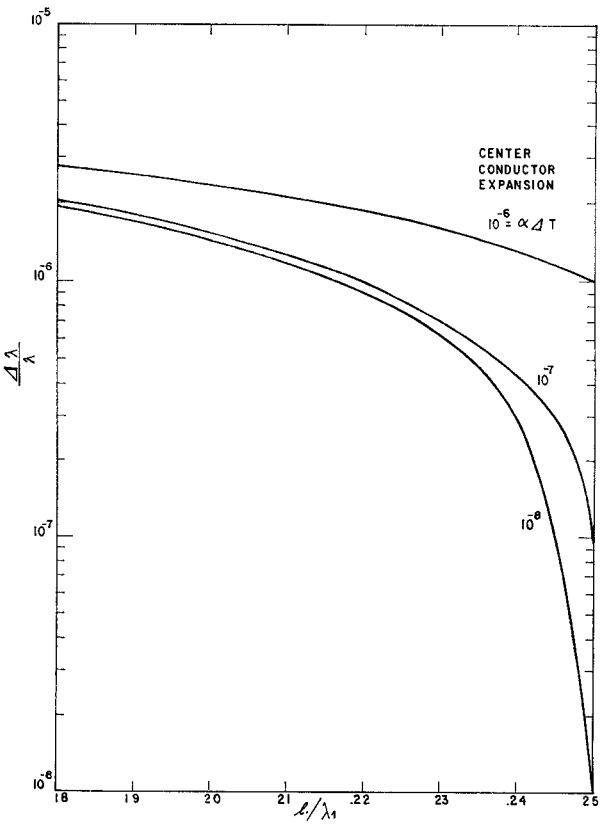

Fig. 5. Stability versus loading for composite coaxial resonator. Brass outer conductor for various inner conductor expansions: $b/a = 3.6$ $a = 0.9$ cm. Outer conductor expansion $= 2 \times 10^{-5}$.

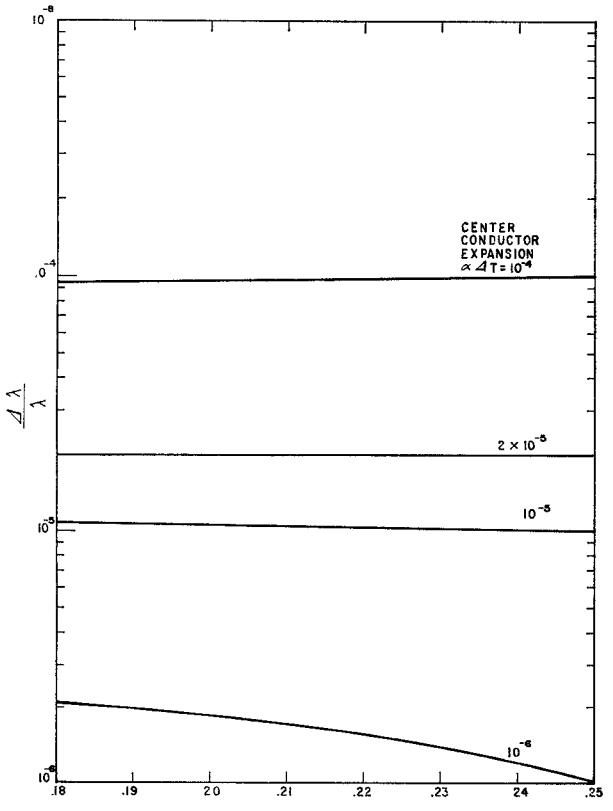

Fig. 6. Stability versus loading for composite coaxial resonator. Brass outer conductor for various inner conductor expansions: $b/a = 9.0$ $a = 0.36$ cm. Outer conductor expansion $= 2 \times 10^{-5}$.

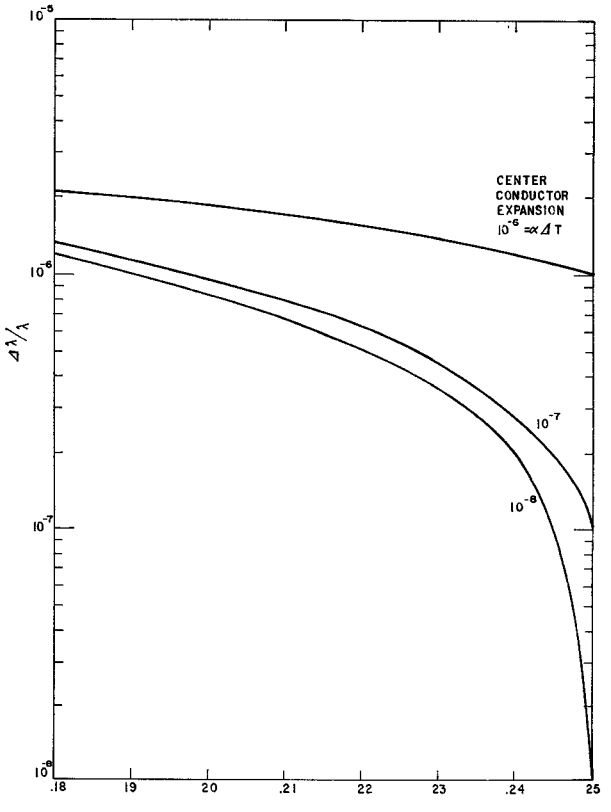

Fig. 7. Stability versus loading for composite coaxial resonator. Brass outer conductor for various inner conductor expansions: $b/a = 9.0$ $a = 0.36$ cm. Outer conductor expansion $= 2 \times 10^{-5}$.

$$\frac{\lambda_1}{kC_1Z} = \tan 2\pi L_1/\lambda_1. \quad (9)$$

For a homogeneous resonator constructed from a single material, the capacitance C_1 changes linearly with temperature while Z remains constant.

$$\left[\tan \frac{2\pi L_1}{\lambda_1}\right] \frac{\lambda_2/\lambda_1}{(1+\alpha T)} = Y_{11} \frac{\lambda_2/\lambda_1}{(1+\alpha T)}. \quad (10)$$

The subscripts 1 and 2 designate the initial and final temperatures, respectively. The solution to (10) occurs when

$$\frac{\Delta\lambda}{\lambda_1} = \alpha \Delta T. \quad (11)$$

Consider the case of a composite resonator constructed from two different materials, say a brass outer conductor and a low-expansion inner conductor. After a change in temperature, ΔT, the resonance condition is described by

$$\tan\left[2\pi \frac{L_1}{\lambda_1}\frac{\lambda_1}{\lambda_2}(1+\alpha(a)\Delta T)\right] = Y_{11}\frac{\lambda_2}{\lambda_1}\frac{C_1}{C_2}\frac{Z_1}{Z_2} \quad (12)$$

where C_1 and C_2 are given by (4) and (5), respectively, and Z_1 and Z_2 are given by (6) and (7). This equation cannot be solved as simply as (10), due to the complex temperature dependence of C_2 and the presence of the impedance term on the right-hand side of the equation.

This equation was solved, using Newton's approximation method, on a digital computer for two conditions. These conditions are for a b/a ratio of 3.6 to 1 with $a=0.9$ cm, and a b/a ratio of 9.0 to 1 with $a=0.36$ cm. The results of these solutions are plotted in Figs. 4–7 for a brass outer conductor and various expansion inner conductors for different initial loading factors. It is evident from the curves that the resonator stability deteriorates rapidly for even slight loading of a resonator with a very low-expansion center conductor. For higher-expansion center conductors, the effect is decreased. For an inner-conductor expansion of 2 parts in 10^5 equal to the brass outer conductor, the stability is equal to the material expansion and independent of the loading as it should be.

Example

A composite coaxial resonator was constructed with a low-expansion center conductor and a brass outer conductor. The diameter ratio was 3.6 to 1 and the radius of the inner conductor was 0.9 cm. At room temperature, resonance occurred at 1.385 GHz compared to an unloaded length corresponding to 1.75 GHz. This is a loading factor l_1/λ of 0.198. Between 25°C and 70°C, the inner conductor had a measured expansion of about 5 parts in 10^7. From Fig. 5, this corresponds to a stability $\Delta\lambda/\lambda$ of 2.2 parts in 10^6. The measured stability of the resonator over this range is 3.8 parts in 10^6. This is good correlation with the small discrepancy possibly due to measurement inaccuracy or additional external influences on the resonator.

L. C. Gunderson
Electronic Research Lab.
Corning Glass Works
Raleigh, N. C.

Isolation of Lossy Transmission Line Hybrid Circuits

I. Introduction

With the advent of integrated microwave circuit techniques, use of lossy transmission lines to achieve miniaturization can seriously affect circuit performance. A frequently used performance characteristic of hybrid circuits is the isolation between conjugate ports. Such isolation is normally limited to maximum values of 40 dB to 50 dB due to incidental mismatch of terminations and capabilities of test equipment. When lossy transmission lines are employed to realize the hybrid circuits, an additional constraint is placed upon the peak isolation that can be achieved. In this correspondence, the theoretical isolations of lossy hybrids will be determined at their design center frequencies. Two different hybrid circuits will be considered: the square hybrid and the "rat race" hybrid ring. The preferred method of analysis of symmetrical four-port networks will be used herein.[1]

To analyze the lossy hybrids, one must use the complex propagation constant γ, where $\gamma=\alpha+j\beta$. The attenuation per unit length is nepers per unit length is α, while β is the phase shift per unit length in radians per unit length. Three trigonometric identities will be used:[2,3]

$$\tanh\left(\frac{\gamma L}{2}\right) = \frac{\cosh(\gamma L)-1}{\sinh(\gamma L)} \quad (1)$$

$$\sinh(\gamma L) = \sinh(\alpha L + j\beta L) = \sinh \alpha L \cos \beta L + j \cosh \alpha L \sin \beta L \quad (2)$$

$$\cosh(\gamma L) = \cosh(\alpha L + j\beta L) = \cosh \alpha L \cos \beta L + j \sinh \alpha L \sin \beta L. \quad (3)$$

For a quarter-wave transmission line of small dissipation, $L=\lambda/4$, $\sinh \alpha L \cong \alpha L$, $\cosh \alpha L \cong 1$, $\sin \beta L \cong 1$, and $\cos \beta L \cong 0$:

Then

$$\left.\begin{aligned} \sinh(\gamma L) &\cong j \\ \cosh(\gamma L) &\cong j\,\alpha L \\ \tanh\left(\frac{\gamma L}{2}\right) &\cong \alpha L + j \end{aligned}\right\}. \quad (4)$$

For a three-quarter-wave transmission line of small dissipation, $3L=3\lambda/4$, $\sinh 3\alpha L \cong 3\alpha L$, $\cosh 3\alpha L \cong 1$, $\sin 3\beta L \cong -1$, and $\cos 3\beta L \cong 0$. Then

$$\left.\begin{aligned} \sinh(3\gamma L) &\cong -j \\ \cosh(3\gamma L) &\cong -j3\alpha L \\ \tanh\left(\frac{3\gamma L}{2}\right) &\cong 3\alpha L - j \end{aligned}\right\}. \quad (5)$$

II. Square Hybrid

The square hybrid (see Fig. 1) uses four quarter-wave transmission lines. The *ABCD* matrix for this hybrid can be found for both the even $(M{+}{+})$ and the odd $(M{+}{-})$ modes:

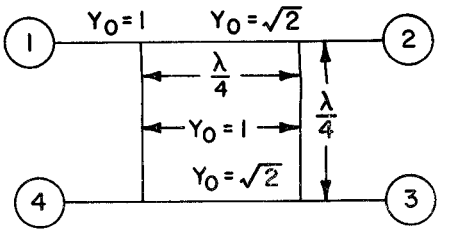

Fig. 1. Square hybrid.

$$M_{+\pm} = \begin{bmatrix} 1 & 0 \\ Y_{+\pm} & 1 \end{bmatrix} \times \begin{bmatrix} \cosh(\gamma_2 L) & \frac{1}{\sqrt{2}}\sinh(\gamma_2 L) \\ \sqrt{2}\sinh(\gamma_2 L) & \cosh(\gamma_2 L) \end{bmatrix} \times \begin{bmatrix} 1 & 0 \\ Y_{+\pm} & 1 \end{bmatrix} \quad (6)$$

where

γ_2 = propagation constant per unit length of transmission lines connecting ports 1 and 2, and ports 4 and 3,

$y_{+\pm}$ are admittances of shunt stubs for even and odd modes.

For the even mode: (shunt stubs are open-circuited)

$$Y_{++} = Y_0 \tanh\left(\frac{\gamma_1 L}{2}\right) \quad (7)$$

where

γ_1 = propagation constant per unit length of transmission lines connecting ports 1 and 4, and ports 2 and 3.

Letting $Y_0=1$, and substituting (4) into (7)

$$Y_{++} = \alpha_1 L + j. \quad (8)$$

For the odd mode: (shunt stubs are short-circuited)

$$Y_{+-} = \frac{Y_0}{\tanh\left(\frac{\gamma_1 L}{2}\right)}. \quad (9)$$

Letting $Y_0=1$ and substituting (4) into (9)

$$Y_{+-} = \frac{1}{\alpha_1 L + j} = \frac{\alpha_1 L - j}{(\alpha_1 L)^2 + 1}. \quad (10)$$

For small dissipation, $(\alpha_1 L)^2 \ll 1$ then

$$Y_{+-} \cong \alpha_1 L - j. \quad (11)$$

Substituting (4), (8), and (11) into (6), it can be shown that

$$M_{+\pm} = j\begin{bmatrix} 1 & 0 \\ \alpha_1 L \pm j & 1 \end{bmatrix} \times \begin{bmatrix} \alpha_2 L & \frac{1}{\sqrt{2}} \\ \sqrt{2} & \alpha_2 L \end{bmatrix} \times \begin{bmatrix} 1 & 0 \\ \alpha_1 L \pm j & 1 \end{bmatrix}. \quad (12)$$

Performing the matrix multiplications in (12) and disregarding all second-order terms involving $\alpha_1 L$ and $\alpha_2 L$:

Manuscript received June 21, 1966; revised September 12, 1966.

[1] J. Reed and G. J. Wheeler, "A method of analysis of symmetrical four-port networks," *IRE Trans. on Microwave Theory and Techniques*, vol. MTT-4, pp. 246–252, October 1956.

[2] J. D. Ryder, *Networks, Lines, & Fields*. Englewood Cliffs, N. J : Prentice-Hall, 1949, p. 200.

[3] *Reference Data for Radio Engineers*, 4th Ed. New York: IT&T Corp., 1956, p. 1949.